Solutions of surfactant oligomers: a model system for tuning foam stability by the surfactant structure

A. Salonen,[a] M. In,[b] J. Emile[a] and A. Saint-Jalmes*[a]

Received 20th November 2009, Accepted 3rd March 2010
First published as an Advance Article on the web 9th April 2010
DOI: 10.1039/b924410g

We report experiments on aqueous foams made of solutions of oligomers of cationic surfactants. The degree of oligomerization is varied up to 4, and two spacer lengths are used. We have studied both the interfacial dilational and shear rheology, the single thin film properties, the foamability of the solutions, as well as the aging and the mechanical properties of the 3D foams. We have found clear differences between the oligomeric systems at all length scales. We then discuss the correlations between the properties at the different length scales and see how the macroscopic features depend on the molecular structure. This work first allows us to determine the relevance of each measurement; in that respect, it stresses the important role of the timescales, and the need to monitor the liquid fraction and bubble size in order to perform correct comparisons. Secondly, this work provides information on how one could optimize foaming properties with oligomers, and the balance between the degree of oligomerization and spacer length.

1. Introduction

An aqueous foam is a dispersion of a gas in a liquid, stabilized by the presence of surfactant molecules adsorbed on the gas–liquid interfaces. The research on foams, both in academia and industry, is very active and covers a variety of aspects: foam rheology, foam stability, foam aging, foam chemistry…[1–5] One of the main reasons for interest in the study of foams is that they are very unusual materials if one simply considers its components (gas and liquid). In fact, the result of the dispersion cannot be seen as a gas, a liquid or a solid, but indeed share some features of these three states of matter, depending on its physico-chemical properties. In that respect, a major issue still to elucidate is where do the macroscopic properties of the foam come from. As a general starting point, one can first claim that the origin of the striking behaviors is the hierarchy of lengthscales, leading to complex coupling between them. Indeed, foams are hierarchically organized at very different lengthscales: the monolayers of surfactant adsorbed at the gas–liquid interfaces (1 nm), the scale of the thin films separating the bubbles (tens of nm), the one of the interconnected liquid channels (called "plateau borders", from tens to hundreds of microns), the one of the bubble size (typically 1 mm) and the macroscopic one. The goal is to determine which specific properties are important at the different lengthscales, and how they infer the macroscopic behavior. It also means that one has to find out what is the balance between the foam's physical and chemical parameters. The physical parameters are essentially the bubble radius, the liquid fraction ε (ε = volume of liquid/volume of foam), the bubble radius polydispersity, and the size and shape of the sample. The chemical ones are linked to the foam stabilizers (molecules adsorbed at the interfaces), the liquid itself (being more or less Newtonian), and the gas. Many types of stabilizers can be used: usual detergent molecules, but also proteins,[6–8] and even solid particles.[5,9,10]

Over the last ten years, there has been some progress on these issues, showing that there can be complex coupling between the lengthscales, and a strong impact of microscopic phenomena on the macroscopic behavior.[4,11,12] But these issues are far from being completely clarified, and many studies show that it is still actually difficult to understand the origins of the properties of the 3D sample, and particularly to relate them to information obtained at different lengthscales.[6–10,13–20] These experimental results generally show that foams behave differently depending on their chemical components; but often the compared systems are so different that unfortunately too many parameters are changed at the same time and at various lengthscales. Moreover, the foam physical parameters, like for instance the size of the bubbles produced, are not always controlled or monitored. Lastly, another difficulty comes from the fact that independent measurements on isolated structures of the foam (single interface, film or bubble) are not necessarily done at the relevant characteristic times and sizes, corresponding to those found inside the 3D foam. Altogether, these difficulties really prevent straightforward comparisons between systems, and elucidating the actual links between lengthscales remains challenging.

To overcome these difficulties, our approach is to systematically screen various and controlled molecular structures, and to perform the same set of controlled experiments at all the possible intermediate lengthscales, up to the macroscopic foam samples. For fine tuning the chemical structures, we use a series of molecules with gradual complexity that can be modified step by step: we start from one surfactant monomer with a single hydrophobic tail, and gradually increase the degree of oligomerization x (up to 4). We then investigate oligomeric surfactants;[21] in addition, we also change the length of the spacer between the attached monomers, with two possible spacer lengths s. Many works on oligomeric surfactants have been

[a]*Institut de Physique de Rennes, Université Rennes 1 - CNRS UMR 6521, Rennes, France. E-mail: arnaud.saint-jalmes@univ-rennes1.fr*
[b]*Laboratoire des Colloïdes, Verres et Nanomatériaux, Université Montpellier 2 - CNRS UMR 5587, Montpellier, France*

This journal is © The Royal Society of Chemistry 2010

done,[21] mostly dealing with their complex bulk structure; however, fewer studies have been performed on the interfacial properties, single films, and up to the scale of the foam, and only with dimeric surfactants.[18–22]

In the following, we first describe the oligomeric surfactants and the methods used to independently scan the features at the different lengthscales. Then, we present the results describing both the interfaces, the films and the foams. Then we analyze these data, and discuss them to try to find the origins of the properties and differences at the intermediate scales. Finally, we also discuss how the foam properties can be tuned and selected by choosing the right type of oligomeric surfactant.

2. Materials and methods

2.1 Foam ingredients: oligomeric surfactant solutions and gas

For the monomeric surfactant, we use two cationic ammonium bromide surfactants, C_nTAB: dodecylTAB with $n = 12$ (DTAB) and tetradedylTAB with $n = 14$ (TTAB) (from Sigma-Aldrich). Then, we have used oligomers of DTAB with the degree of polymerization x varied from 2 to 4 and the spacer length s equal to 3 or 6. We finally performed measurements with two dimers (($x = 2$, $s = 3$) and ($x = 2$, $s = 6$)), two trimers (($x = 3$,$s = 3$) and ($x = 3$,$s = 6$)) and one tetramer (($x = 4$)), with two spacer lengths following the sequence 12-3-12-4-12-3-12). The molar mass of all the molecules are given in the Table 1.

The different molecules are synthesized following the procedure described in ref. 22. All the molecules were dissolved in Millipore water. We have used two different gases: air and perfluorohexane C_2F_6, in order to tune the gas diffusion and foam coarsening rates (see section 2.4).

2.2 Intermediate-scale studies: interfaces and films

We have used a palette of complementary methods, for both gaining information on the statics and dynamics of the interface. The dynamics of the adsorption at the interface is measured by the rising bubble method (Tracker apparatus from Teclis). The same technique, in oscillatory mode, provides measurements of the dilational viscoelastic moduli, E'_s and E''_s. The frequency of the oscillations is varied from 0.02 to 0.2 Hz, and the amplitude is kept constant at 0.05.

For the viscoelastic response to shear, we have used a biconical setup adapted on a MCR 301 Paar Rheometer. The edge of the bicone is placed at the interface with high precision, such that only the interface is sheared. Such measurements give the interfacial shear elastic and loss moduli, G'_s and G''_s. The frequency of the oscillations is between 0.01 and 10 Hz, and the amplitude can be varied from 0.01 to 0.5. Still on the gas-liquid interfaces, we also investigated the texture and spatial organization by Brewster Angle Microscopy. These interfacial experiments are performed at 20 ± 2 °C.

Further experiments have been performed with the "thin film balance" apparatus.[23,24] This setup allows us to study a single thin film, held horizontally on a glass circular support (using a Scheludko-type cell[24]). By videomicroscopy, one can then determine the film uniformity and homogeneity, and the thickness can be determined by interferometry. By increasing the

Table 1 Summary of results including information on the molecules, on the bulk solution, on the interfacial and foam properties. The time t_a is the characteristic adsorption time and γ_{eq} is the interfacial tension at equilibrium. The frequency f_c is the crossover frequency corresponding to $E'_s = E''_s$. Values of these viscoelastic dilational moduli are also given at a fixed frequency of 0.1 Hz. G' (t = 0) is the bulk elastic modulus of the foam

Molecule	Molar mass/g mol^{-1}	CMC/M	γ_{eq}/mN m^{-1}	t_a/s	f_c/Hz	Int. dil. rheo. $f = 0.1$ Hz	Foamability	Stability drainage coarsening	G' (t = 0)/Pa
DTAB	308	14.2×10^{-3}	39.7	<1	—	$E'_s \sim E''_s \sim 0$	Poor	—	—
TTAB	336	3.5×10^{-3}	38.5	<1	—	$E'_s \sim E''_s \sim 0$	Optimal	Classical	20
$x = 2$, $s = 3$	628.7	0.96×10^{-3}	32.7	<1	—	$E'_s \sim E''_s \sim 0$	Optimal	Classical	28
$x = 2$, $s = 6$	670.8	1.0×10^{-3}	39.4	<1	—	$E'_s \sim E''_s \sim 0$	Optimal	Classical	—
$x = 3$, $s = 3$	949	0.14×10^{-3}	33	90	0.015	$E'_s \sim 80E''_s \sim 37$	Medium—pore size dependant	Enhanced stability—slower drainage and coarsening	41.5
$x = 3$, $s = 6$	1033.2	0.26×10^{-3}	40.1	4.5	0.3	$E'_s \sim 9E''_s \sim 19$	Medium—pore size dependant	Enhanced stability + collapse	—
$x = 4$	1283.4	5.9×10^{-4}	36.6	7000	—	$E'_s \sim 140E''_s \sim 28$	Poor	—	—

This journal is © The Royal Society of Chemistry 2010

pressure on the film, one can reproduce the same effect as inside a foam under drainage.

2.3 Foamability and foam studies

For the foam production and foamability measurements, we have used a bubbling method: it consists of blowing gas into porous glass frits immersed in the surfactant solution. The gas rate and the frit porosity are controlled and varied: we have used porosity from no.1 (pore size = 100–160 μm) to no.4 (pore size = 10–16 μm), and the range of gas injection rate is 0.1–1 L min^{-1}. The foam cell in Plexiglas has a square section of 2 × 2 cm, a height of 30 cm and is open at the top. All the foam experiments are performed at 20 ± 2 °C.

The characteristic of good foaming (high foamability) is that all the injected gas is incorporated inside the foam, leading to a uniform bubble distribution, with a controlled size. In that case, the foaming parameter ξ, defined as the volume of foam V_f divided by the volume of gas injected V_g,[25] becomes independent of the bubbling time (after some transient regime) and $\xi \approx 1$. Note that if the foams are wet and contain a large amount of liquid (>20%), then $\xi \geq 1$. In the case of intermediate foaming (medium foamability), the bubble diameter is found bigger than expected, as a consequence of film rupturing and coalescence already occurring during the bubbling. In that case, some foam can still be produced, but at a slower volume production rate, as some gas escapes out of the foam ($0.25 < \xi < 1$). Finally, for bad foaming (poor foamability) almost no foam is created, and the destruction rate is similar or faster than the production one ($\xi < 0.25$). Also, one gets very strong fluctuations of the liquid fraction in time and space, with holes in the foam. So, by visual observation and monitoring the height of foam, we have a way to classify the ability of the solution to foam. In Fig. 1 (a,b,c) are examples of foams—using the same frit porosity—at high (a), medium (b) and low (c) foamability.

For good foamability and homogeneous foams (as in Fig. 1a), we can subsequently monitor the foam aging (time zero for aging is set after the arrest of bubbling). First, its drainage is measured by electrical measurements: pairs of electrodes (Fig. 1 (d,e)) are embedded in the cell walls in order to obtain $\varepsilon(z,t)$ (using the calibration curves provided in ref. 26). The evolution of the bubble size, either due to coarsening or to bubble rupturing, is followed by direct imaging of the bubbles at the surface of the container (examples are given in Fig. 1 (f,g,h)). Though for optical reasons, this is not ideal for absolute estimation of the bubble size, it is still well-suited for a relative measurement and for comparisons between samples within a series.

For foam rheology, we have used the MCR 301 rheometer (Anton-Paar), in a plate-plate configuration (the gap is 2 or 3 mm). The foams are made by the bubbling method with porosity no.4 (high liquid fraction, and fast rate of gas, leading to bubble diameter of a few hundreds of microns, depending on the oligomers used). Once produced, the sample is placed directly within the plate-plate setup of the rheometer, and the elastic and viscous foam moduli, G' and G'', are measured under small oscillations. Typical frequency-sweeps and amplitude-sweeps are then performed.[3,27]

2.4 Foam models: time evolution and rheology

Beside the chemical composition, an aqueous foam is characterized by two physical parameters: the liquid fraction ε and the average radius of the bubbles R. Both evolve with time: the variation of ε is due to drainage and variation of R is due to coarsening and film rupturing.

We briefly recall here the basic theoretical aspects of foam drainage. In the situation of free-drainage (ε_0 uniform at $t = 0$, over a height H), the liquid fraction at a given height z, $\varepsilon(z,t)$ is constant during a time τ, and then it decreases with a power law: $\varepsilon(t) \sim t^{-\alpha}$. The exponent α varies between 1 and 2 depending on the interfacial mobility.[4,11,28] The interfacial mobility describes the coupling between flow within the plateau borders and inside their interfaces; it turns out that the relevant microscopic interfacial parameter involved in this coupling is the interfacial shear viscosity,[4,11] which depends on the surfactants used. The time τ corresponds to the time required for a drying front (which starts

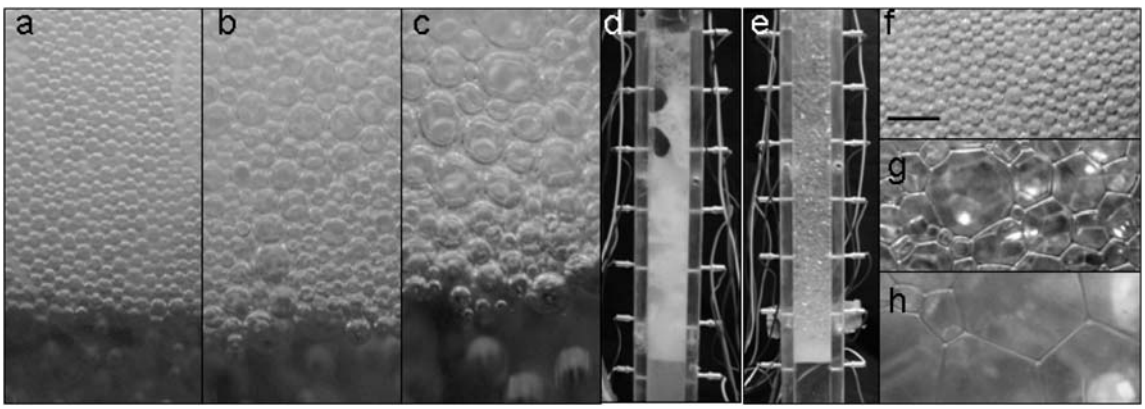

Fig. 1 Typical pictures of the foams. (a), (b) and (c): pictures during foam generation, where the picture width is 4 mm. In the three cases, the frit porosity is identical (porosity 4), but the solutions are changed; resulting in differences in the foam, illustrating good (a) and bad (c) foamability (the solutions are, respectively, TTAB, ($x = 3$, $s = 3$) and ($x = 4$)). (d), (e): front view of the foam column, with the electrodes installed on both sides used to measure the electrical conductance and to determine the local liquid fraction. The column height is 30 cm. In (d), the foam collapses rapidly after foam production; while in (e), the foam structure is very stable and the foam has drained and coarsened without spontaneous film ruptures; (f), (g) and (h): close-up of the same foam, at three different times. With time, the bubble size grows (coarsening). Bar length = 1 mm.

at the top of the sample) to reach a position z. This time increases as one goes down into the sample. It is also possible to determine a typical velocity describing the speed of the liquid inside a foam, for constant bubble size and liquid fraction ε:[28]

$$V = K\frac{\rho g R^2}{\mu}\varepsilon^{\beta} \quad \text{(Eqn 1)}$$

Here K is a dimensionless prefactor, β is an exponent between ½ and 1, ρ is the fluid density, g is the gravitational acceleration and μ is the fluid viscosity. The parameters K and the value of β depend again on the interfacial mobility, as discussed before for the exponent α. Using eqn (1) and considering a column of height H, a typical timescale for drainage is:

$$t_d = \frac{\mu H}{K\rho g R^2 \varepsilon^{\beta}} \quad \text{(Eqn 2)}$$

This time corresponds to the time needed for 1/2 (or 2/3) of the total volume of liquid to have leaked out of the foam (case $\beta = 1$ and $\beta = 1/2$, respectively).

Foams also age by coarsening: this effect is due to the diffusion of gas from bubbles (the smallest ones, with a low number of faces) to the large ones (having a large number of faces).[28,29] As a consequence, the number of bubbles with time decreases and the mean size increases. In the usual model, the process is considered as self-similar,[29,30] implying that:

$$\left(R^2(t) - R_0^2\right)/R_0^2 = \frac{t}{t_c} \quad \text{(Eqn 3)}$$

In that case, the bubble radius (equal to R_0 at $t = 0$) grows asymptotically in $t^{1/2}$. One can also write the coarsening time as:

$$t_c = \frac{R_0^2}{D_{eff} h(\varepsilon) f(\varepsilon)} \quad \text{(Eqn 4)}$$

This time incorporates an effective diffusion coefficient D_{eff}, containing the gas properties (diffusivity and solubility) and the gas–liquid interfacial tension.[31] The thickness of the film separating the bubbles is h, which is also a function of the liquid fraction (here, $h(\varepsilon)$ is a function normalized by the minimal thickness h_0 found in the limit of ε tending to zero). Lastly, one must also take into account a function $f(\varepsilon)$, describing the effective area of a bubble covered by thin films and through which gas diffusion occurs.[31] Note that eqn (4) stands for a constant liquid fraction in time. Foam coarsening is a slow process, tuned by the gas diffusion, and thus the gas properties. This is different from film rupturing: both lead to the bubble size increasing but not *via* the same origin. Coarsening occurs in all foams, even the most stable; while film rupturing is the signature of poor foam stability. In that respect, the first one leads to a self-similar distribution of sizes, while film rupturing leads to inhomogeneities and holes.

Drainage and coarsening can be strongly coupled: as seen in eqn (2) and 4, the timescales are valid for either constant bubble diameter or constant liquid fraction. If R or ε changes during these timescales, *i.e.* drainage and coarsening are simultaneous, a strong coupling occurs resulting in a synergistic effect, which makes both drainage and coarsening faster.[4,31] This makes the study of the elementary processes involved in foam aging quite difficult.

Concerning foam rheology, the previous experimental works show that the elastic modulus G', once normalized by the Laplace pressure, γ/R, is a simple function of the liquid fraction:[27]

$$G'/(\gamma/R) \sim (1 - \varepsilon)(\varepsilon_c - \varepsilon) \quad \text{(Eqn 5)}$$

The critical value ε_c corresponds to the vanishing of elasticity found when the bubbles are no longer compressed.[3,27] Eqn (5) means that G' decreases both with the bubble radius R, and with ε. It also means that the chemicals only play a role *via* the surface tension γ. Though it is usually valid for foams made of low molecular weight surfactants, this is not the case for emulsions where high interfacial compression elasticity E' and low interfacial tension can provide a situation where the foam elastic modulus G' is controlled by E', rather than by γ.[32]

3. Results

In this section, we first present the results of the foam properties: we present whether or not the solutions foam and what are the properties of the produced foams. Then, we present the results of the foam sub-structures, what we have learned from the interfaces and from the films.

3.1 Foam results

Foamability. We performed foaming tests at concentrations equal to 2 times the critical micellar concentration (cmc) for all the systems. We have decided to use high concentrations of oligomers above the cmc, so that one can be sure that all the interfacial properties have reached their saturation limits and do not depend on concentration anymore: in that respect, all the following experiments at every length scale are done at 2 cmc. The cmc values have been measured and are given in section 3.2 and in Table 1.

The foaming experiments showed that the solutions of the different oligomers do not foam the same way. For the dimers, we have found good foamability and $\xi = 1$, whatever the porosity (as in Fig. 1a). In contrast, the solutions of trimers are much more difficult to foam, which is even more marked for the spacer

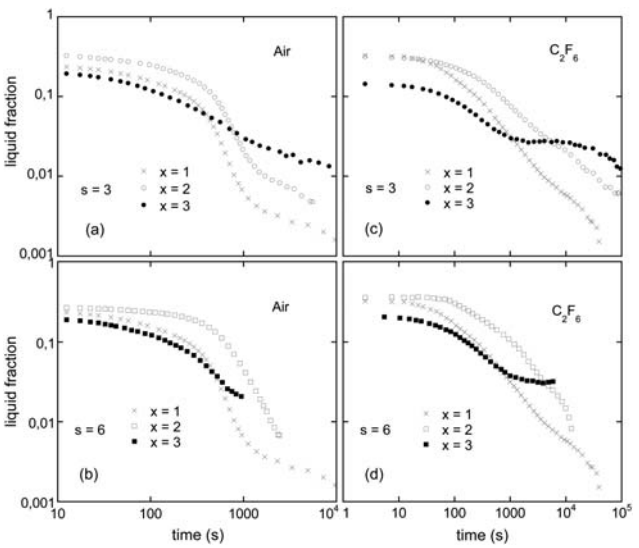

Fig. 2 Liquid fraction in the foam as a function of time, at a given position (in the middle of the column), for the two gases and five solutions: TTAB (×), ($x = 2, s = 3$) (○), ($x = 2, s = 6$) (□), ($x = 3, s = 3$) (●), ($x = 3, s = 6$) (■).

This journal is © The Royal Society of Chemistry 2010

$s = 3$. In fact, only with the smallest porosities (no. 3 and 4), can a foam be produced, but with relatively large bubbles ($R_0 = 350$ μm, and about twice as big as the dimers with porosity no. 4), meaning poor incorporation of gas (Fig. 1b), and ξ does not ever exceed 0.6. The worst foamability is found for the tetramers, and it is impossible to get even very coarse and unstable foams ($\xi <$ 0.1). Note lastly that there is almost no effect of the gas properties (air or C_2F_6) on the foamability. A summary of the results is also given in Table 1.

Foam aging. For the cases where the solution has good enough foamability and no film rupturing during foaming, we have investigated the drainage and coarsening of the foam. Fig. 2 shows the time evolution of the liquid fraction at the same vertical position ($z = 10$ cm from the bottom liquid interface) for the foams made using the different molecules and the two gases. Results are given for the same frit porosity (porosity 3) and the same gas rate. Varying these parameters does not change the qualitative features described below. The two graphs on the left (right) are for air (C_2F_6) foams; similarly, the top (bottom) graphs compile the results for $s = 3$ (6). Finally in each graph, the results for various x (1, 2 and 3) are shown. It is important to note that we use here TTAB, rather than DTAB for the case $x = 1$, as DTAB solutions alone have a too low foamability for clean drainage and coarsening measurements (without bubble coalescence).

A few general statements can be made: first, drainage is always slower with the C_2F_6; secondly, the maximum value of the liquid fraction found after bubbling—ε_0—is different from system to system, despite the use of the same porosity, and lastly, the one with the highest ε_0 is the last to start draining. If one looks in more detail, for the dimers ($x = 2$) and whatever s, the results are similar to the TTAB ones: after a time τ, where the liquid fraction remains constant, a first power law decrease is observed, with exponent α (as defined in section 2.4) being -1.8 ± 0.2. At longer times, slower dynamics are observed (for $t >$ 1000 s in Fig. 2a), leading towards a fully drained foam and liquid fractions well below 1%.

With ($x = 3$, $s = 3$), the situation is more complex, and we observe an inflexion and almost a plateau along the curve (clearly seen in Fig. 2c); in that part, the exponent α is <0.5. The situation looks a bit similar for the trimer ($x = 3$, $s = 6$) with the same drainage deceleration, but it also includes another feature: the films finally rupture inside the foam, and the foam eventually collapses. This foam collapse occurs at time $t = 950$ s for air (Fig. 2b), and $t = 8000$ s for C_2F_6 (Fig. 2d), both corresponding to a critical liquid fraction of 0.02–0.04.

Fig. 3 shows the evolution of the normalized bubble size as a function of time. Here, the same frit porosity is used for all the samples, meaning that the mean initial radii vary from 150–200 μm ($x = 1$ and $x = 2$) to 350–400 μm (for $x = 3$). For air and for C_2F_6, the main features of R/R_0 are similar: the curves are simply shifted towards longer times for C_2F_6. The major difference between the systems is that for short spacer trimer ($x = 3$, $s = 3$), the rate of coarsening turns out to be more than a decade slower than for the others.

Foam rheology. The time evolution of the viscoelastic moduli G' and G'', measured in the limit of small oscillations (frequency $f = 1$ Hz, amplitude $\delta = 0.01$) are reported in Fig. 4. The graph compares the data for TTAB, the dimer ($x = 2$, $s = 3$) and the trimer ($x = 3$, $s = 3$). The experiments for DTAB and $s = 6$ are not performed because the foams were too unstable for rheometrical measurements (as also found in Fig. 2b). On one hand, concerning the elastic modulus, we have found that the value at $t = 0$—G'_0—increases with the degree of oligomerization (see Table 1). Comparison with eqn (5) will be done in section 4. There might also be a difference in their rate of decrease: a slower decay for the dimers and trimers is found. On the other hand, the

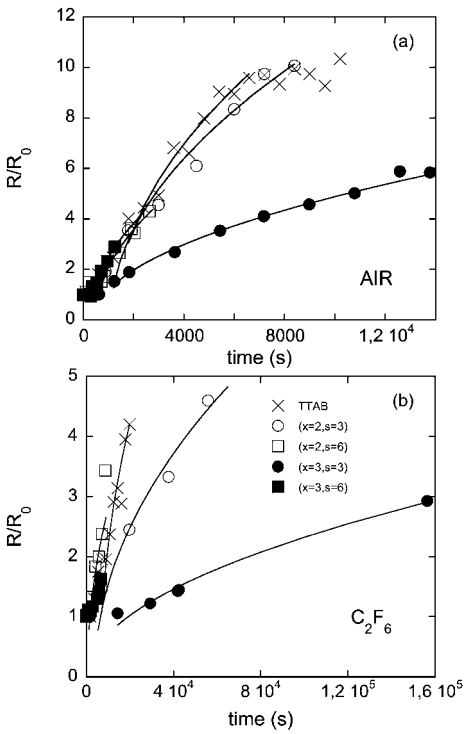

Fig. 3 Normalized bubble radius *vs.* time for the foams prepared using air and C_2F_6. The lines are fits, following the model discussed in the text.

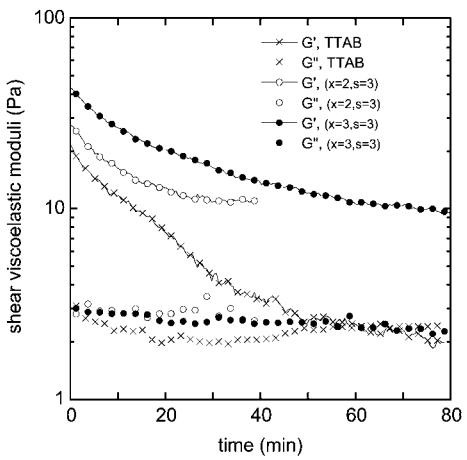

Fig. 4 Foam elastic modulus G' and viscous modulus G'' as a function of time, for foams made of TTAB and the oligomeric surfactant solutions (with $s = 3$). The plate–plate separation is 3 mm.

viscous moduli are all close at $t = 0$, and it seems that there is less decrease with the oligomers than with the monomer.

3.2 Interfacial results

We have measured the equilibrium interfacial tension of the dimer and trimer solutions as a function of their concentrations. Such measurements have first allowed us to determine the critical micellar concentrations (cmc) of each system. We have found results in agreement with previous works:[22] the values of the cmc and of the equilibrium surface tension γ_{eq} are listed in the Table 1. For the following measurements, as already stated, we have used high concentrations of oligomers, above their cmc (note that they are very different between the molecules).

At such concentrations, Fig. 5 shows the surface tension for the different solutions as a function of time. We observe strong differences between the molecules, and the variation of the spacer s and degree of oligomerization x have decoupled effects. On one hand, x acts only on the timescales: the higher the degree of oligomerization, the slower the adsorption. On the other hand, s acts both on the final value of the tension γ_{eq} (independently of x), and on the timescales: the shorter the spacer, the slower the adsorption and the lower the final tension. For all the trimers and tetramers, we can extract a typical adsorption time, t_a, values of which are compiled in Table 1.

A very interesting feature with short spacer surfactant oligomers, is that we can get low values of surface tension γ ($\sim$35 mN m^{-1}) meaning significant amounts of absorbed materials (at least when compared to a naked interface), but with very slow dynamics; usually, slow dynamics corresponds to low concentrations of surfactant, and thus high final surface tension at equilibrium with almost no matter adsorbed at the interfaces.

The results of dilational viscoelasticity are presented in Fig. 6, where the elastic and loss moduli are plotted as a function of the oscillatory frequency f. We have first found that, in the range of frequencies available, there is no viscoelasticity for the interfaces covered by the dimers ($x = 2$), $E'_s = E''_s \approx 0$. For the trimer ($x = 3$, $s = 6$), the interface is more viscous than elastic within the range of frequencies available ($E'_s < E''_s$ in Fig. 6a). It seems that both moduli will become equal at slightly higher frequencies; we can extrapolate that the interface will become more elastic than viscous at frequencies higher than a crossover frequency f_c being

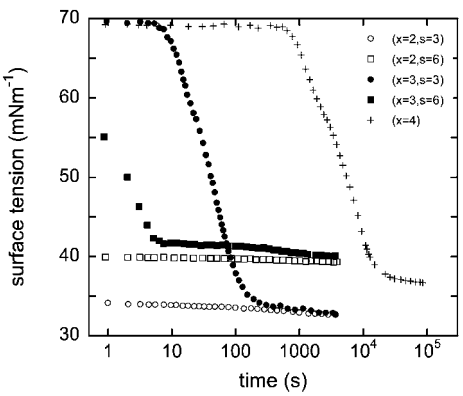

Fig. 5 Surface tension *vs.* time for the five oligomeric solutions, all at 2 cmc. Note the large differences in adsorption timescales.

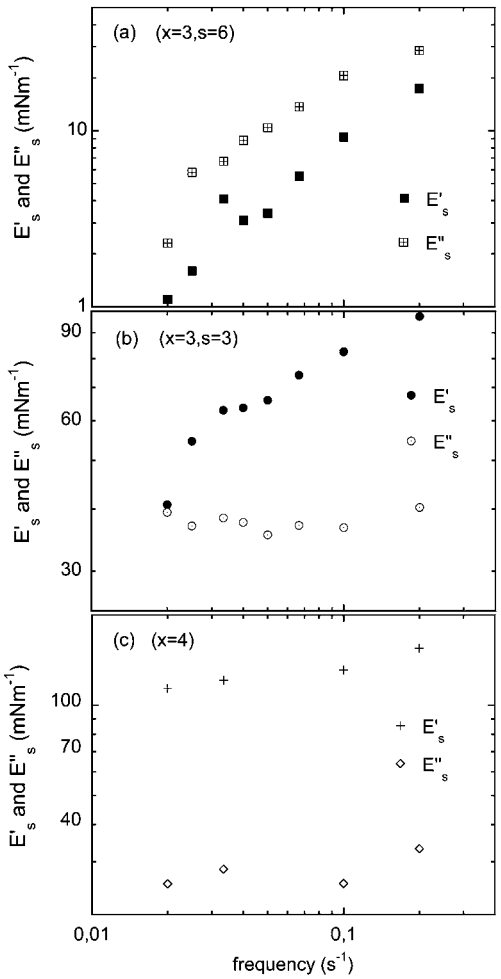

Fig. 6 Interfacial viscoelastic dilational moduli E'_s and E''_s as a function of the dilational frequency.

of the order of 0.3 Hz. With the smaller length of the spacer (Fig. 6b), the crossover between elastic and viscous is clearly observed, though we can just reach the limit frequency at which E''_s becomes similar to E'_s (at $f_c \approx 0.015$ Hz). Lastly, for $x = 4$, the crossover is shifted to such low values of f that it cannot be measured by our apparatus, and E'_s is always larger than E''_s (Fig. 6c). Note also the very high values of E'_s for the trimer ($x = 3$, $s = 3$) and for the tetramers ($x = 4$) (>50 mN m^{-1}); these are values not often found in the literature at these low frequencies, meaning that the layers are indeed strongly elastic. So, depending on x and s, one can get either an interface having very high dilational elasticity (dominating viscous contributions), or a viscoelastic interface where viscous contributions dominate, or practically no viscoelasticity at all (for the dimers and the monomers).

Concerning the shear viscoelasticity, these interfaces turn out to be always fluid-like: first, the apparatus never detects an elastic contribution; secondly, the values for G''_s are always close to the limit of resolution and typically equal to those found for monomeric surfactants ($G''_s \leq 10^{-5}$ Pa m). Lastly, using Brewster Angle Microscopy, we also learn that there are no in-plane structures at the interfaces, even under compression. The monolayers are thus always uniform, without domains or segregation.

This journal is © The Royal Society of Chemistry 2010

3.3 Film and bulk results

All the thin films observed by the thin film balance share the same main properties; they all belong to the range of "black films" (equilibrium thickness $h < 100$ nm), and are spatially uniform. Nevertheless, we have found a stratification phenomenon[24] for the trimer ($x = 3$, $s = 6$): the film is spatially organized in thickness, and as it is put under pressure (to mimic the capillary suction inside a draining foam) a layer of micelles is expelled due to its confinement inside the film. The other films do not show stratification. We also want to point out that the films for the trimer ($x = 3$,$s = 3$) have much slower dynamics towards equilibrium: flows inside the films are strongly slowed down when compared to the other molecules.

In the bulk, the surfactant solutions all have the same Newtonian viscosity $\mu = 10^{-3}$ Pa s, as determined in a double-gap cylindrical Couette geometry. This confirms the previous works, where it was shown that μ remains low at these concentrations. Nevertheless, it is known that it increases drastically with concentration.[21,22,33]

Lastly, note that the molecules assemble in supramolecular assemblies, and the shape of these structures is known to depend on the degree of polymerization and spacer. In particular, the dimer ($x = 2$, $s = 3$) and trimer ($x = 3$, $s = 3$) form elongated and cylindrical micelles,[22] but the latter are found generally at concentrations higher than those used here. Note though that—already at these low concentrations—there are also large differences in terms of aggregation numbers (numbers of monomers inside the micelles) with the degree of oligomerization.

4. Data analysis and discussion

We have found strong variations between the molecular systems at the interface, as well as clear differences in the foamability, foam drainage and foam coarsening, and probably also, but less significantly, in foam rheology. In this section, we verify first if the results obtained with each individual molecule at all scales can be understood in terms of molecular structure, then if they are consistent with each other and finally if the different macroscopic features can be explained with the molecular origins.

First, we focus on the scale of the interfaces. The dynamics of the surface tension are correlated to the size of the molecules and to their charge. Two factors can contribute to the slowing down of the adsorption and to the increase of the time t_a: the bigger the molecule, the lower the diffusion coefficient in the bulk, and trimers and tetramers may take longer times to migrate from the bulk to the vicinity of the interface. Moreover, the different values of the cmc can also partially explain the dynamics; there are fewer and fewer molecules as we go from monomers to tetramers. However, the bulk to interface diffusion and the value of the cmc are not the only mechanisms controlling the adsorption dynamics of such oligomers, since it would lead to a slower adsorption of the trimer ($x = 3$, $s = 6$) as compared to ($x = 3$, $s = 3$). In that respect, it is not trivial to understand the effect of the spacer length: increasing s makes the adsorption faster, but the surface tension γ_{eq} at the interface is higher. Other effects like electrostatic barriers must be taken into account for these systems:[34] as ionic surfactants approach the air/water interface, they are going to get repelled by their image charge (because of the dielectric constant contrast between air and water). In fact, preliminary measurements of adsorption rate with added salt show that the dynamics are actually strongly accelerated and that the differences diminish when electrostatic repulsions are screened. The local charge density is higher for short spacer trimers than for large spacer ones and may explain the slower adsorption of ($x = 3$, $s = 3$). The differences could also be due to the type of aggregates in the bulk: there are spherical micelles for $s = 6$ and more complex and elongated shapes for $s = 3$, possibly implying a slower adsorption process. Moreover, the aggregation number is larger for $s = 3$, resulting also in a slower adsorption rate. In contrast, it seems that the packing at the interface is still better with $s = 3$: the lower value of γ_{eq} is then a consequence of a smaller effective area per molecule.[35] The non-trivial dependence of the dynamics $\gamma(t)$ (timescale, shape of the curve, effect of added salt) with the concentration and parameters x and s will be discussed in another article, including measurements of the interfacial concentrations.[22]

We also want to point out that there are good correlations between the dilational viscoelasticity and surface tension dynamics. For the two trimers, the crossover frequency f_c—at which the interface shifts from solid-like to fluid-like (Fig. 6)—corresponds well to the inverse of the adsorption time t_a (see Table 1). This means that the viscoelastic properties of the interfacial layers are only controlled by the adsorption/desorption of the molecules. This is further confirmed by the fact that we have measured no contributions in shear, meaning that there are no in-plane structures or bonds (in contrast to protein layers, for instance, where usually both dilational and shear properties are coupled and change together). For ($x = 4$), we cannot have access directly to f_c (Fig. 6c); but, following the results for the trimers, we can extract from Fig. 5 and the values of t_a, that f_c is 1500 times smaller than for ($x = 3$, $s = 6$), and equal to $f_c = 2 \times 10^{-4}$ Hz.

We can further push our analysis on these interfacial issues. Ideally, if one could have the full curves for $E'_s(f)$ and $E''_s(f)$ and for all of the molecules, one could test if the microscopic

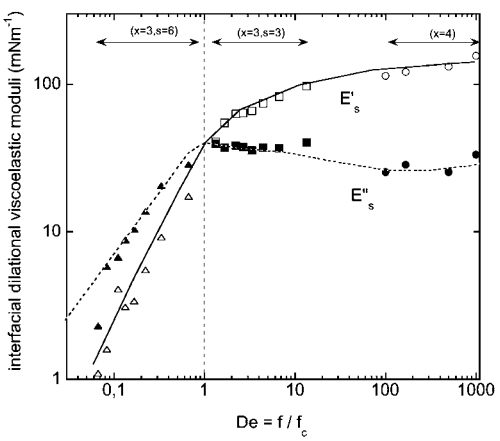

Fig. 7 Rescaling of the results of Fig. 6, illustrating the "molecule-frequency" superposition approach. The whole curves of E'_s and E''_s are built—piece by piece—by re-scaling the results obtained in a small frequency window with different oligomers. Lines are guides for the eyes. De is a dimensionless Deborah number.

mechanisms responsible for the viscoelasticity are the same: by re-scaling the experimental frequency by f_c, one just has to test whether all the data get superposed on the same master curves of E'_s and E''_s. In that spirit, we can separately rescale the frequency of the three sets of data of Fig. 6 by their respective f_c, and plot them on the same graph with f/f_c as the x-axis (Fig. 7).

On one hand, as we can only collect data in a small range of frequencies, the result of Fig. 7 cannot really confirm a collapse of all the data onto two master curves. But, on the other hand, if one assumes that this frequency re-scaling is valid, this approach turns out to be a way to create, piece by piece, the two curves of $E'_s(f)$ and $E''_s(f)$ on much larger ranges than what is experimentally accessible (more than 4 orders of magnitude in Fig. 7). This re-scaling actually corresponds to a "molecule/frequency" superposition method, exactly similar to the classical "temperature/frequency"[36] or "shear-rate/frequency" superposition.[37] Indeed, the overall shapes of the curves which can be extrapolated (lines on Fig. 7) look reasonable and consistent with other measurements of viscoelastic moduli as a function of frequency.[37] Note also that there is no need for vertical shift. The dimensionless ratio f/f_c, corresponding to t_a/t, can be identified as a Deborah number, De: for $De > 1$, elastic contributions dominate, and it is the opposite for $De < 1$. Though the curves of Fig. 7 look rather convincing, it is still necessary to investigate in more detail this "molecule/superposition" method, to fully confirm that it is equivalent to performing either a measurement with a single oligomer over a wide range of frequencies, or measurements in a small window of frequencies but with different oligomers. This would require larger experimental frequency ranges, or other values of x and s. At this stage, this analysis of the dilational viscoelastic data show that this family of oligomers indeed appears as a model interfacial system, since changing x or s only acts quantitatively on the timescales of adsorption/desorption (t_a and f_c), while only these adsorption/desorption mechanisms control and are at the origin of the viscoelasticity.

After the discussion at the scale of a single interface, we can then look at the foamability results. Looking at the dynamics of adsorption, one can understand that the dimers are foaming well: a rapid surface tension decrease leads to fast bubble stabilization. However, it is surprising that the trimer solutions do foam: obtaining a low surface tension and a significant amount of molecules adsorbed at the interface (at least, when compared to a naked interface) requires tens of seconds, while the time for a bubble to rise straight from the frit towards the liquid foam is only of a couple seconds. However, during the foaming process, there is a lot of turbulence, and the bubbles are frantically shaken. This increases the residence time of a bubble in the bulk. Also, it helps to maintain high concentrations of surfactant close to the bubble interface. The situation is thus very different from the tranquil rising bubble configuration. Due to this bubble shaking, there can be a much faster rate of adsorption. This effect is also confirmed by the dependence on the porosity: when trying to make large bubbles, the use of large pore sizes reduces the mixing and shaking of bubbles inside the fluid, thus the foamability of the solution can change with the preparation. In the opposite case, the effect is limited: even in the presence of strong shaking of the bubbles (with small frit pores), it is impossible to foam the tetramer solution, and even the increased adsorption obtained by mixing is not enough in this case to finally provide any sufficient adsorption at the interfaces (needed to produce disjoining pressures between the bubbles). This clearly confirms the link between foamability and rapid adsorption at the interface; knowing that rapid is relative to the timescale of the foaming method and that the foaming method itself has also an impact on the adsorption dynamics. One could then wonder about the use of the $\gamma(t)$ curve for foamability issues, since—in the usual quiescent setup—it cannot take into account the effects produced by the foaming process. However, we have seen that it gives interesting information on foamability in the way that it can help to sort solutions between those which will easily foam and those which will require at least strong injection of energy. These measurements are also important for understanding what are the mechanisms controlling the adsorption (diffusion, electrostatic barrier, etc…)[34] and for investigating the origins of the dilational viscoelasticity (purely controlled by the interface/bulk exchange—as here, or with an intrinsic contribution from within the layer itself).

Concerning the foam stability and aging (when there is a good foamability), it turns out that we can separate between features which can be explained within the usual theoretical framework of drainage and coarsening, and new surprising results. For instance, it is normal that the liquid fraction ε_0 is maximal for the dimers: good foamability means the production of small bubbles, which in turn implies high fluid content brought inside the foam during the bubbling time (as drainage is slow (eqn (1))). Consequently, the drainage is slow during production (high ε), but also after the arrest of bubbling during free drainage: this explains why the dimers are the last curves to start to decrease. These are all classical results, not related to complex coupling, if one carefully understands that the differences in foamability result in different initial bubble size. The same argument is valid for the initial value ε_0 obtained for the trimer solutions: low foamability means larger bubble sizes, and thus a smaller ε_0, implying both a faster drainage and a decay arising sooner (eqn (1)–(2)).

However, there are surprising results for the two trimers along the drainage curves. As described previously, a plateau is seen for the trimer ($x = 3$, $s = 3$), followed by a re-acceleration of drainage (Fig. 4c), and finally resulting in an outstanding stability of this foam in time. Similarly, it seems that a plateau could occur for ($x = 3$, $s = 6$), but the foam collapses at the same time, preventing the observation of the same behavior as for the trimer ($x = 3$, $s = 3$).

In fact, none of the existing drainage models can explain these features. We can first rule out an effect due to the interfacial rheology. Within the usual models (eqn (1)–(2)), the shear interfacial properties play a role, but only through the value of K and the exponent β; even drastic variations of the shear viscoelasticity cannot provide such a behavior; moreover, as shear rheometry showed, there are no differences between the systems since all the moduli G'_s and G''_s always remain very low. The impact of the dilational viscoelasticity on foam drainage is less understood than the effect of the shear viscoelasticity; indeed, the dilational viscoelastic moduli are not taken into account in eqn (1) and 2, but they still might play secondary roles *via* effects linked to the Marangoni effect.[11] Nevertheless, it also seems difficult to draw a link between the slowing down of the drainage rate with time and the constant dilational elasticity of the

 This journal is © The Royal Society of Chemistry 2010

interfaces. However, as discussed below, it could play a more important role on the coarsening rates.

Having ruled out the effects due to the interfacial rheology, a possible explanation could be that the deceleration of drainage rate and the constant value of ε are linked to the gradual jamming of the fluid inside the network of plateau borders, as already seen for foams of colloidal solutions.[38] As the foam drains, the section of the plateau borders decreases: the confinement inside these narrow channels might result in a local increase of the viscosity. This could be especially expected with the trimer ($x = 3$, $s = 3$) which is known to make elongated micelles, which could become more and more entangled under confinement. So, it seems that the very good stability in time of these trimer ($x = 3$, $s = 3$) foams could be a consequence of their supramolecular structure inside the fluid. This interpretation is supported by the observation of the single thin films where the drainage dynamics, directly seen on microscopy, is strongly slowed down.

The same mechanism could be possible for the trimer ($x = 3$, $s = 6$), but it seems to be finally covered by another effect which breaks the films and the foam. Again here, the observations of the single thin film are complementary. As described before, for the trimer ($x = 3$, $s = 6$), the films undergo a thickness jump down to a very thin thickness under pressure; such increase of pressure in the thin film apparatus indeed corresponds to the same situation as inside a draining foam, where the suction on the films from the plateau borders increases as the foam drains. After the stratification and the expulsion of a layer of micelles, the thin films of trimer ($x = 3$, $s = 6$) always continue to thin, down to a thickness of less than 20 nm, and become unstable. Thus, the trimer ($x = 3$, $s = 6$) can stabilize rather wet foams (*i.e.* low capillary suction from the plateau borders on the films); but as soon as there is too much suction (*i.e.* low liquid fraction, $\varepsilon < 0.05$), the films are thin and eventually get too fragile. In that respect, an important difference between the two trimer foams is the existence or not of stratification inside the films, leading to faster or slower film thinning. For the systems studied here, despite strong differences in the interfacial properties, the foam features seem to be more controlled by phenomena and structures inside the bulk solution, rather than at the bubble interfaces. The continuous thinning down to thickness less than 20 nm observed for the film of trimer ($x = 3$, $s = 6$) could also be correlated to a specific feature of the molecules in bulk. As also found for polysoap molecules, there is a wide gap of miscibility and the solutions are diphasic at concentration as low as 3% (and up to 60%).[39] The origin of this effect—not seen for the other trimer ($x = 3$, $s = 3$)—is the possible bridging between micelles by molecules, providing attractive forces and phase separation. In that respect, one could speculate that such attractive interactions between adsorbed interfaces could also be at the origins of the continuous thinning of the trimer film, leading to their rupture.

At this stage, it is interesting to look at the coarsening results ($R/R_0(t)$ in Fig. 3) in the light of the drainage results. We find that—after some time t'—the data can be adjusted by the model of eqn (3). The delay t' corresponds to the time where the liquid fraction changes strongly due to drainage: after t', the foam is almost fully drained, and the liquid fraction is no longer changing rapidly with time. It is reasonable to find, in agreement with eqn (3), that the model can roughly describe the data once the liquid fraction has reached an almost constant value. In fact, with these foams, because the initial liquid fraction is quite high at the beginning (>0.25), drainage is fast while coarsening is initially slow (eqn (1)–(2)); in a crude picture, the foams mostly drain first, and they mostly coarsen once they are dry.

Fig. 3 also shows that there is a much slower coarsening for ($x = 3$, $s = 3$). The difference in the initial bubble size cannot fully explain this effect (eqn (4)). In fact, the differences between the initial bubble diameters vanish rapidly as the foams do not coarsen all at the same initial rate, so that after a few minutes the bubble diameters are finally all equivalent. Then, qualitatively, it is tempting to link this slow coarsening to the high interfacial dilational elasticities found in Fig. 6b, as discussed in ref. 40. But, to get a real impact of the elastic modulus, it still has to be large at the relevant frequency, the one corresponding to the coarsening rate. Here, foams coarsen very slowly, with typical coarsening times of 10^3–10^4 s (Fig. 4 and eqn (4)), and we have seen that at long times (low frequencies) the dilational viscoelasticity always vanishes (Fig. 7). So we have to check if the rates of interfacial area variations $\mathrm{d}A/\mathrm{d}t$ performed in the rising bubble apparatus, and leading to the results of Fig. 3b, are in the same range as those inside the foam. From Fig. 3, it turns out that inside the foam we get typically $\mathrm{d}A/\mathrm{d}t \sim 0.7\text{–}3 \times 10^{-3}$ mm^2 s^{-1}, while with the drop oscillation frequency, we get $\sim 10^{-3}$–10^{-2} mm^2 s^{-1}. The ranges are close, though we remain experimentally limited and are not able to measure at sufficiently low enough rates of area change. It is thus difficult to conclude whether or not the elastic modulus is still significantly high inside the foam. Looking at the shape of the master curves in Fig. 7, one can be sure that the moduli have decreased to smaller values than in Fig. 6b (at least, closer to the value of the surface tension) at the relevant frequencies inside the foam. These results cannot confirm a strong and direct correlation between the dilational viscoelastic moduli and the rate of coarsening; nevertheless, the interfacial elasticity probably plays a role, especially here for the trimer ($x = 3$, $s = 3$), but it is probably not the only origin of the observed slower coarsening.

In fact, beside the possible role of the interfacial elasticity, the apparently slower coarsening of the trimer foams ($x = 3$, $s = 3$) is also a consequence of the slower drainage and of the high constant value of ε. As recalled previously, coarsening strongly depends on the liquid fraction ε (eqn (4)). If ε remains high (compared to a fully drained foam) the coarsening will be slower, mostly because of the function $f(\varepsilon)$ in eqn (4). In that respect, our most anomalous result is seen in the drainage curves (Fig. 2a,c), but finally not in the coarsening (Fig. 3): the latter can just be a consequence of the drainage, being itself a possible consequence of effects in the bulk (like entanglement of micelles inside the fluid network). This illustrates clearly how erroneous conclusions could easily be drawn if one forgets to compare data at the same liquid fractions.

Lastly, still concerning the origins of the outstanding stability of the ($x = 3$, $s = 3$) foams (at least when compared to the others), we also have to take into account the strong coupling between drainage and coarsening, as they both depend on R and ε. If it is true—as proposed before—that the slower coarsening is a consequence of the slower drainage (eqn (4)), one must also add that this slower coarsening itself has an impact on the drainage rate and prevents it increasing (by keeping R small).

Thus, altogether, it appears that the behavior of the trimer ($x = 3, s = 3$) foams comes both from the reduced drainage (due to bulk effects), the reduced coarsening (due to interfacial effects), and from the coupling of these two effects which enhance both of them.

We can then wonder if a clear signature of the high dilational elasticity seen in Fig. 6 is found in the macroscopic features. The rheological tests of Fig. 4 possibly give a positive answer, especially the high value of G'_0 found for ($x = 3$, $s = 3$). It turns out that the value of G'_0 agrees with eqn (5) for TTAB, meaning that the one for the trimer ($x = 3$, $s = 3$) is thus anomalously high (even more anomalous when the scaling with the bubble diameter is taken into account). Here, the oscillation frequency of the rheometrical measurement $f = 1\ s^{-1}$, and falls within the range where E'_s is actually large and well above the surface tension γ for the trimer ($x = 3, s = 3$). As found for emulsions, it seems that we have here, for the first time, a foam for which the main elastic contribution is no longer associated with γ but with E'_s; thanks to the oligomerization, the adsorption–desorption dynamics have been slowed down such that, at the frequencies probed, the interfacial layer has no time to relax and the trimer molecules can be considered as almost insoluble.

5. Conclusions

We have obtained a new set of data on well-controlled solutions of oligomers of cationic surfactant and on their foams. Measurements on all of the foam sub-structures and up to the 3D foam have clearly shown that the oligomer solutions have very different interfacial, film and foam properties, and that the foam properties depend on the nature of the chemicals used. Two types of conclusions can be made: general ones on the link between scales in foams which are illustrated by these studies, and more specific ones on this family of molecules and their use as foaming agents.

A first general statement—valid in the case of molecules with slow adsorption dynamics, arising from high adsorption barriers—is that the more difficult it is to make the foam, the more stable it will be afterwards (if it can be produced). If the stabilizer adsorption requires a lot of energy, desorption of these adsorbed species will also be difficult, with high energy barriers to desorption. Such reluctance to desorb will induce high interfacial viscoelasticity and will slow down the coarsening, which can even be completely stopped as in the case of particle-stabilized foams.[10]

Another general statement is that the link between interfacial properties and bulk are definitively not trivial, and that the differences observed between samples are not necessarily linked to differences at the interfaces. On such issues, the timescales are crucial, and one needs to fully characterize the foam conditions, especially the liquid fraction, to extract correlation between lengthscales. Otherwise there are many risks to make mistakes by ascribing an effect to a wrong cause: our analyses show that many possible links between the scales could have been proposed *a priori*, but that many can finally be discarded once it becomes clear that direct comparisons were not possible (not the same bubble size, or liquid fraction, or the same timescales). In this spirit, it also becomes clear that adapting the experimental protocols and methods of fabrication to get fixed initial liquid fraction and bubble size, whatever the chemical system, is a better approach than simply performing experiments with a fixed fabrication method. Though this does not appear impossible, it requires a lot of tests to adjust the experimental production method to the system foamability in order to obtain the desired foam parameters.

Nevertheless, some clear correlations between properties at different lengths can be identified thanks to this family of oligomers: between $\gamma(t)$ and foamability, between a single film stability and the 3D foam stability, between bulk structure and foam stability and drainage, and between interfacial dilational viscoelasticity and foam coarsening and rheology.

On the latter, if the dilational viscoelasticity has to play a role on a specific process, it first must be significant at the characteristic frequency of the given process. At long times (low frequency), for such soluble molecules, the elasticity has always fully vanished. However, this interfacial elasticity may play a role for rheology: oscillatory frequency can be comparable to adsorption/desorption processes, rate of rearrangements, *etc.* One can also expect that it could play a role in the film rupturing processes at high frequencies.

Another way of extracting global conclusions from these results is to come back to the issue of equilibrium between physical and chemical parameters in foams. Clearly, our results show that quantitatively there is always a strong dependence with the bubble size and the liquid fraction, and that the chemical components can have an effect by the way they act on the time evolution of R and ε.

The second type of conclusion deals directly with the oligomers of surfactant. It turns out that these molecules are very efficient for foaming when compared to the DTAB monomer (which almost does not foam). They also appear as a very interesting model system for many reasons: first, because their viscoelasticity results only from the bulk-interface exchange, without in-plane structure and interaction; secondly, because they bring the crossover frequency f_c to a frequency range much more relevant for foams. With a usual low molecular weight surfactant, f_c is much higher ($\sim 10^3$ Hz). Thus, one can think about enhancing or reducing an effect based on interfacial mobility by using the right oligomers: interfaces can be either solid-like or fluid-like, and this can be tuned by the degree of polymerization. Another advantage of using members of such a family for fundamental investigation is that one remains with pure and simple systems, rather than making complex formulations. Lastly, there are many degrees of freedom: one can either play with x or s; thus, this can be optimized depending on the properties required. Clearly there is fundamental interest in creating and understanding the behavior of new surfactant structures, which will lead to increased control in the design of new types of dispersed materials (foams, emulsions, *etc.*) with specific desired properties.

6. Acknowledgments

The authors thank financial support from the ANR (ANR-BLAN – 07 – 340), and V. Vié for performing the BAM experiments.

References

1 R. K. Prud'homme, S. A. Khan, *Foams: Theory, Measurements, and Applications*, Marcel Dekker Inc. New York, 1997.
2 A. Saint-Jalmes, D. J. Durian, D. Weitz, *Kirk-Othmer Encyclopedia of Chemical Technology*, 5th edn, 2005, 8, John Wiley and Sons, New York, p. 697.

 This journal is © The Royal Society of Chemistry 2010

3 R. Hohler and S. Cohen-Addad, *J. Phys.: Condens. Matter*, 2005, **17**, R1041.
4 A. Saint-Jalmes, *Soft Matter*, 2006, **2**, 836.
5 S. Tcholakova, N. D. Denkov and A. Lips, *Phys. Chem. Chem. Phys.*, 2008, **10**, 1608.
6 A. H. Martin, K. Grolle, M. A. Bos, M. A. Cohen-stuart and T. van Vliet, *J. Colloid Interface Sci.*, 2002, **254**, 175.
7 J. P. Davis and E. A. Foegeding, *Colloids Surf., B*, 2007, **54**, 200.
8 T. Croguennec, A. Renault, S. Bouhallab and S. Pezennec, *J. Colloid Interface Sci.*, 2006, **302**, 32.
9 B. P. Binks, *Curr. Opin. Colloid Interface Sci.*, 2002, **7**, 21; B. P. Binks and T. S. Horozov, *Angew. Chem., Int. Ed.*, 2005, **44**, 3722.
10 A. Cervantes Martinez, E. Rio, G. Delon, A. Saint-Jalmes, D. Langevin and B. P. Binks, *Soft Matter*, 2008, **4**, 1531.
11 H. A. Stone, S. A. Koehler, S. Hilgenfeldt and M. Durand, *J. Phys.: Condens. Matter*, 2003, **15**, S283.
12 ND. Denkov, V. Subramanian, D. Gurovich and A. Lips, *Colloids Surf., A*, 2005, **263**, 129; S. Tcholakova, ND. Denkov, K. Golemanov, KP. Ananthapadmanabhan and A. Lips, *Phys. Rev. E: Stat., Nonlinear, Soft Matter Phys.*, 2008, **78**, 011405.
13 H. Fruhner, K. D. Wantke and K. Lunkenheimer, *Colloids Surf., A*, 2000, **162**, 193.
14 A. Colin, J. Giermanska-Khan, D. Langevin and B. Desbat, *Langmuir*, 1997, **13**, 2953.
15 D. Langevin, *Adv. Colloid Interface Sci.*, 2000, **88**, 209.
16 A. Bhattacharyya, F. Monroy, D. Langevin and F. F. Argillier, *Langmuir*, 2000, **16**, 8727.
17 W. Xu, A. Nikolov, D. T. Wasan, A. Gonsalves and R. P. Borwankar, *Colloids Surf., A*, 2003, **214**, 13.
18 A. Pinazo, L. Perez, M. R. Infante and E. Franses, *Colloids Surf., A*, 2001, **189**, 225.
19 A. Espert, R. v. Klitzing, P. Poulin, A. Colin, R. Zana and D. Langevin, *Langmuir*, 1998, **14**, 4251.
20 D. P. Acharya, J. M. Guttierez, K. Aramaki, K. I. Aratani and H. Kunieda, *J. Colloid Interface Sci.*, 2005, **291**, 236.
21 R. Zana, *Adv. Coll. Int. Sci.*, 2002, **97**, 203.
22 M. In, V. Bec, O. Aguerre-Charriol and R. Zana, *Langmuir*, 2000, **16**, 141.
23 V. Bergeron, *J. Phys.: Condens. Matter*, 1999, **11**, R215.
24 C. Stubenrauch and R. von Klitzing, *J. Phys.: Condens. Matter*, 2003, **15**, R1197.
25 A. Saint-Jalmes, M. L. Peugeot, H. Ferraz and D. Langevin, *Colloids and Surface A*, 2005, **263**, 219.
26 K. Feitosa, S. Marze, A. Saint-Jalmes and DJ. Durian, *J. Phys.: Condens. Matter*, 2005, **17**, 6301.
27 S. Marze, R. M. Guillermic and A. Saint-Jalmes, *Soft Matter*, 2009, **5**, 1937.
28 S. A. Koehler, S. Hilgenfeldt and H. A. Stone, *Langmuir*, 2000, **16**, 6327.
29 S. Jurine, S. Cox and F. Graner, *Colloids Surf., A*, 2005, **263**, 18.
30 D. J. Durian, D. A. Weitz and D. J. Pine, *Phys. Rev. A: At., Mol., Opt. Phys.*, 1991, **44**, R7902.
31 S. Hilgenfeldt, S. A. Koehler and H. A. Stone, *Phys. Rev. Lett.*, 2001, **86**, 4704; K. Feitosa and D. J. Durian, *Eur. Phys. J. E*, 2008, **26**, 309.
32 T. Dimitrova and F. Leal-Calderon, *Langmuir*, 2001, **17**, 3235.
33 M. In, G. G. Warr and R. Zana, *Phys. Rev. Lett.*, 1999, **83**, 2278.
34 H. Diamant and D. Andelman, *Langmuir*, 1994, **10**, 2910.
35 M. In in *Reactions and Synthesis in Surfactant Systems*, ed. J. Tetxer, vol. 100, Surfactants Science Series, M. Dekker Inc., 2001, pp. 59–110.
36 J. Heijboer, *Kolloid-Z.*, 1956, **148**, 36; J. D. Ferry, *Viscoelastic properties of polymers*, Wiley, New York, 3rd edn, 1980.
37 H. M. Wyss, K. Miyazaki, J. Mattsson, Z. Hu, D. R. Reichman and D. A. Weitz, *Phys. Rev. Lett.*, 2007, **98**, 238303.
38 R. M. Guillermic, A. Salonen, J. Emile and A. Saint-Jalmes, *Soft Matter*, 2009, **5**, 4975.
39 M. In and R. Zana, *J. Dispersion Sci. Technol.*, 2007, **28**, 143.
40 D. Georgieva, A. Cagnat and D. Langevin, *Soft Matter*, 2009, **5**, 2063.